DEPARTMENT OF MECHANICAL ENGINEERING AND MECHANICS
COLLEGE OF ENGINEERING AND TECHNOLOGY
OLD DOMINION UNIVERSITY
NORFOLK, VIRGINIA 23529

CONSERVATIVE FINITE VOLUME SOLUTIONS OF A LINEAR HYPERBOLIC TRANSPORT EQUATION IN TWO AND THREE DIMENSIONS USING MULTIPLE GRIDS

By

Monchai Kathong

and

Surendra N. Tiwari, Principal Investigator

Progress Report
For the period ended June 30, 1987

Prepared for the
National Aeronautics and Space Administration
Langley Research Center
Hampton, Virginia 23665

Under
Cooperative Agreement NCC1-68
Dr. Robert E. Smith, Technical Monitor
ACD-Computer Applications Branch

July 1987

DEPARTMENT OF MECHANICAL ENGINEERING AND MECHANICS
COLLEGE OF ENGINEERING AND TECHNOLOGY
OLD DOMINION UNIVERSITY
NORFOLK, VIRGINIA 23529

CONSERVATIVE FINITE VOLUME SOLUTIONS OF A LINEAR HYPERBOLIC TRANSPORT EQUATION IN TWO AND THREE DIMENSIONS USING MULTIPLE GRIDS

By

Monchai Kathong

and

Surendra N. Tiwari, Principal Investigator

Progress Report
For the period ended June 30, 1987

Prepared for the
National Aeronautics and Space Administration
Langley Research Center
Hampton, Virginia 23665

Under
Cooperative Agreement NCC1-68
Dr. Robert E. Smith, Technical Monitor
ACD-Computer Applications Branch

Submitted by the
Old Dominion University Research Foundation
P.O. Box 6369
Norfolk, Virginia 23508

July 1987

FOREWORD

This is a progress report on the research project "Numerical Solutions of Three-Dimensional Navier-Stokes Equations for Closed-Bluff Bodies," for the period ending June 30, 1987. Specific attention has been directed to investigate the "Conservative Finite Volume Solutions of a Linear Hyperbolic Transport Equation in Two and Three Dimensions Using Multiple Grids." This work was supported by the NASA/Langley Research Center (Computer Applications Branch, Analysis and Computation Division) through the cooperative agreement NCC1-68. The cooperative agreement was monitored by Dr. Robert E. Smith of the Computer Applications Branch, ACD.

CONSERVATIVE FINITE VOLUME SOLUTIONS OF A LINEAR HYPERBOLIC TRANSPORT EQUATION IN TWO AND THREE DIMENSIONS USING MULTIPLE GRIDS

By

M. Kathong[1] and S.N. Tiwari[2]

ABSTRACT

The feasibility of the multiple grid technique is investigated by solving linear hyperbolic equations for simple two- and three-dimensional cases. The results are compared with exact solutions and solutions obtained from the single grid calculations. It is demonstrated that the technique works reasonably well when two grid systems contain grid cells of comparative sizes. The study indicates that use of the multiple grid does not introduce any significant error and that it can be used to attack more complex problems.

[1] Graduate Research Assistant, Department of Mechanical Engineering and Mechanics, Old Dominion University, Norfolk, Virginia 23529.

[2] Eminent Professor, Department of Mechanical Engineering and Mechanics, Old Dominion University, Norfolk, Virginia 23529.

TABLE OF CONTENTS

LIST OF TABLES

TABLE OF CONTENTS (Concluded)

LIST OF FIGURES

1. INTRODUCTION

In recent years much progress has been made in the solutions of steady state equations of motion in both two and three dimensions. For complex shapes these calculations are usually based on a body-fitted curvilinear grid. For general three-dimensional bodies (for example, an aircraft configuration), it is very difficult to construct a body-fitted coordinate system [1]*. To simplify this problem, it is becoming more common to use several grids (multiple grids) at once, each in a different coordinate system [2-4]. This approach results in new boundaries within the given region at the interfaces of the various grids (Fig. 1.1). In order that information be transferred from one grid to another accurately, it is important to treat grid points on the interfaces with care. The non-linear nature of the equations of motion permits solutions with discontinuities such as shocks and slip surfaces. In order that such discontinuities assume the right strength and physical location, it is imperative that the scheme used for the calculations be conservative [5]. In a multiple grid calculation, it is important that the interfaces are also treated in a conservative manner so that the discontinuities can move freely across these interfaces.

The question of conservation when switching between two different grids or numerical schemes has been considered by several authors. Warming and Beam [6] derived transition operators for switching conservatively between MacCormack's method and a second order upwind scheme. Hessenius and Pulliam [7] applied this transition operator approach to derive so-called zonal

*The numbers in brackets indicate references.

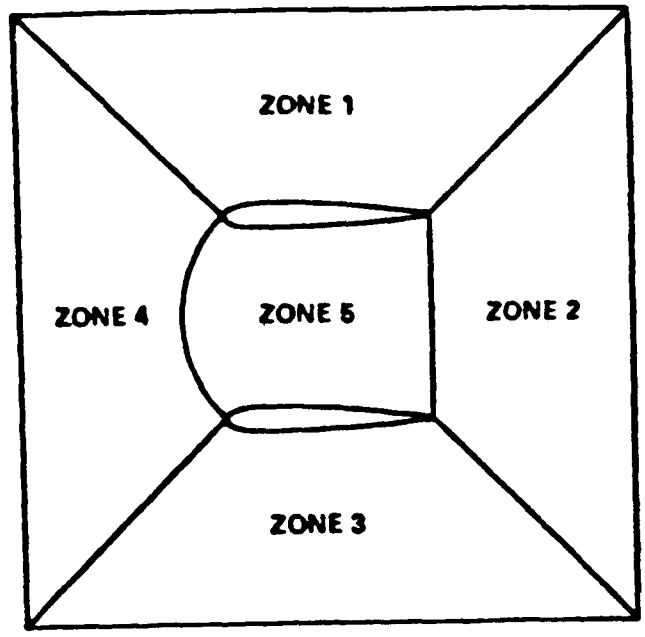

Fig. 1.1. Zoning of multiply connected region.

interface conditions, but with a significant loss of accuracy at the zonal interfaces. Rai [8] has developed conservative zonal interface conditions for zonal grids which share a common grid line, and has nice calculations demonstrating the shock capturing ability of zonal grids with a discontinuity crossing zones. Earlier work in the area of multiple grids includes that of Cambier et al. [9] who analyzed the zonal-boundary problem for a system of hyperbolic equations and used the compatibility equations to develop a zonal-boundary scheme. Good results are presented for transonic channel flow. However, the use of the compatibility equations results in a zonal-boundary scheme that is not conservative and, hence, unsuitable for problem in which flow discontinuities move from one grid to another. Rai et al. [10] present results obtained on metric discontinuous grids; the integration scheme used is the Osher upwind scheme. Reference 11 gives results obtained on overlaid grids in conjunction with the stream function approach. For more information on multiple grid one should refer to [12-20]. the need for conservative grid interfaces is illustrated by Benek, Steger, and Doughtery [3].

Dukowicz [21] described a rezoning method for arbitrary quadrilateral meshes in two dimensions. Ramshaw [22] suggested a procedure which is similar to the method of Dukowicz, but is simpler and more direct. Note that they defined rezoning as a method for transferring a conserved quantity, Q, from one generalized mesh to another when the volumetric density of Q is uniform within each cell of the original mesh. A computer program which follows Ramshaw's procedure has been written and tested with various types of grids and variables. The program seems to be working well. The objective of this study is to establish whether or not this technique is feasible for various grid systems while keeping the governing equation simple.

For simplicity, the scalar 2D and 3D hyperbolic equations are chosen for this study. Hyperbolic equations have had a history of being used as model equations for testing newly developed schemes, for example, see [23-30]. Finite volume approach is chosen along with three-stage Runge-Kutta time integration. The three-stage Runge-Kutta integration is of 2nd order accuracy. Many authors have applied the finite volume approach and Runge-Kutta to their numerical calculations [38-42].

This study can be divided into two portions. First, the scalar 2D hyperbolic equations, $q_t + aq_x + bq_y = 0$ is considered. Here, the equation is solved on a two dimensional grid system which is changed into another grid system at some time, say $t = t_1$. The information obtained from the first grid calculation is transferred to the second grid by Ramshaw's technique. Many authors, for example Berger [43], suggested that in order to retain the conservative property of the numerical scheme, the interpolation of flux across the interface is needed. For this problem, q itself is the flux. Ramshaw's technique is used to transfer q across the interface. The second portion of this study is to examine the technique with the scalar 3D hyperbolic equation, $q_t + aq_x + bq_y + cq_z = 0$. This equation is more suitable as the model equation of the equations of motion. Here, the grid system is changed from one to another at some $x = y$ plane, say plane $z = z_1$. Plane z_1 is the interface mentioned previously. For this problem, the flux is going through this plane, i.e., flux in z direction = $h = cq$, needs to be transferred across the plane. Again, Ramshaw's technique is implemented in doing so. Details and procedures of solving both 2D and 3D hyperbolic equation is given in later sections. The results are compared with exact solutions and solutions obtained from the single grid calculations, i.e., without applying the Ramshaw's technique. It is important to note that

the objective of this study is to determine whether the technique is applicable for these simple governing equations. If it is applicable, one may have some confidence that it will be applicable for more complicated equations. It is expected that the results from this study will yeild a significant contribution in the area of Computational Fluid Dynamics.

In Sec. 2, a brief discussion on Ramshaw's technique is given. Sections 3 and 4 are concerned about the two and three dimensional hyperbolic equation, respectively. Finally, the conclusion is given in Sec. 5.

2. DISCUSSION ON CONSERVATIVE REZONING ALGORITHM

Rezoning is a method for transferring a conserved quantity Q from one generalized mesh to another when the volumetric density of Q is uniform within each cell of the orginial mesh. The need for rezoning was discussed in Sec. 1. A rezoning method for arbitrary quadrilateral meshes in two dimensions has recently been described by Dukowicz [21]. Ramshaw [22] suggested the procedure in doing so which is similar in spirit to the method of Dukowicz, but is simpler and more direct. A computer program following this procedure has been written and is working well for example grids and a wide variety of choice of variables.

By far the most common type of generalized mesh is the arbitrary quadrilateral mesh, which is convenient to work with because it has the same simple topological and logical structure as a square or rectangular mesh. the basic idea behind the rezoning is simple. Here, two grid systems are overlapped each other in some fashion (Fig. 2.1). The conserved quantity, denoted by Qo_{kl}, is to be transferred from the old grid system (Ao_{kl} is the area of each mesh in the old grid system) to the new grid system in which

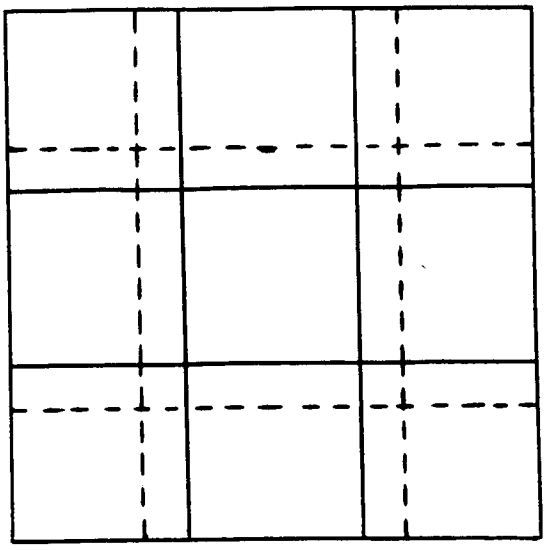

Fig. 2.1(a). Overlapped Grids

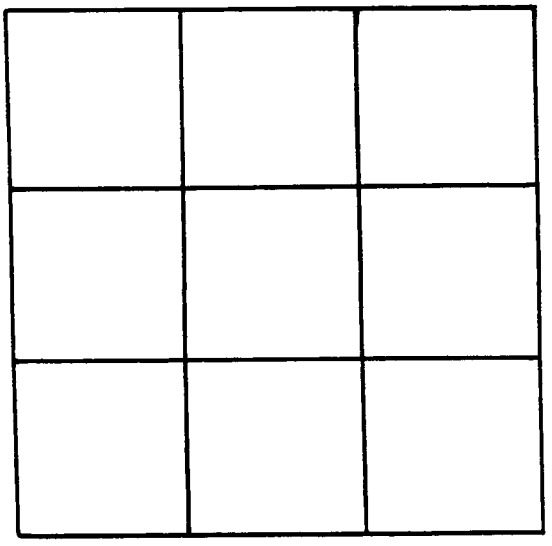

Fig. 2.1(b) Old Grid with known Q_{okl}

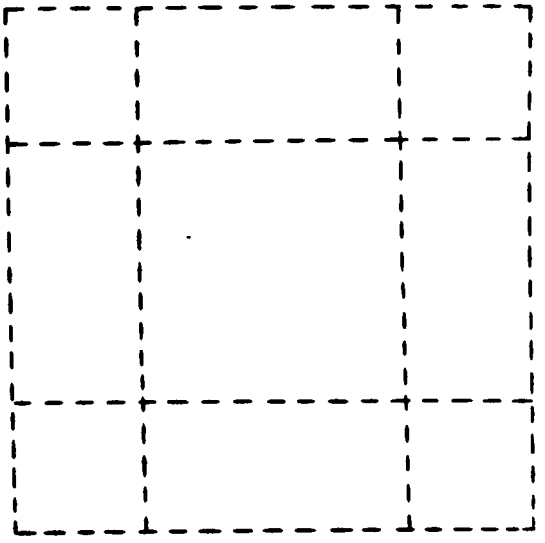

Fig. 2.1(c). New Grid with unknown $Q_{n_{ij}}$

An_{ij} is the area of each. The quantity Qn_{ij} is denoted as the transferred quantity in each mesh of the new grid system. Thus, Qn_{ij} can be computed by:

$$Qn_{ij} = \Sigma(Qo_{kl}) \frac{(Ano_{kl})}{Ao_{kl}} = (qo_{kl}) (Ano_{kl})$$

where $An_{o_{kl}}$ is the portion of the area An_{ij} which is contained in the area Ao_{kl}, and the summation is up to the number of the old meshes contained in An_{ij}. The quantity $q_{okl} = Qo_{kl}$ represents the volumetric density of Qo_{kl} and is assumed to be uniform within each cell. The task, now, is to find Ano_{kl} and the number of the old meshes contained in each An_{ij}. The area of the polygon P is given by [44]

$$A_p = \frac{1}{2} \sum_s \varepsilon_s^p (x_1^s y_2^s - x_2^s y_1^s),$$

where the summation is over all the sides of P, and ε_s^p is either +1 or -1 depending on whether P lies to the left or right of side s. Note that the endpoint coordinates (x_1^s, y_1^s) and $(x_2^s, y^s{}_2)$ are considered to be associated with the side s and not with the particular polygon P.

Figure 2.2 shows arbitrary overlap grids. The overlap areas are polygons whose sides are segments of the old-mesh lines. The number of sides of each type, and total number of sides, will be different for different overlap areas. Each side is common to two overlap areas, the one on the left (L) and the one on the right (R), and these overlap areas may be considered

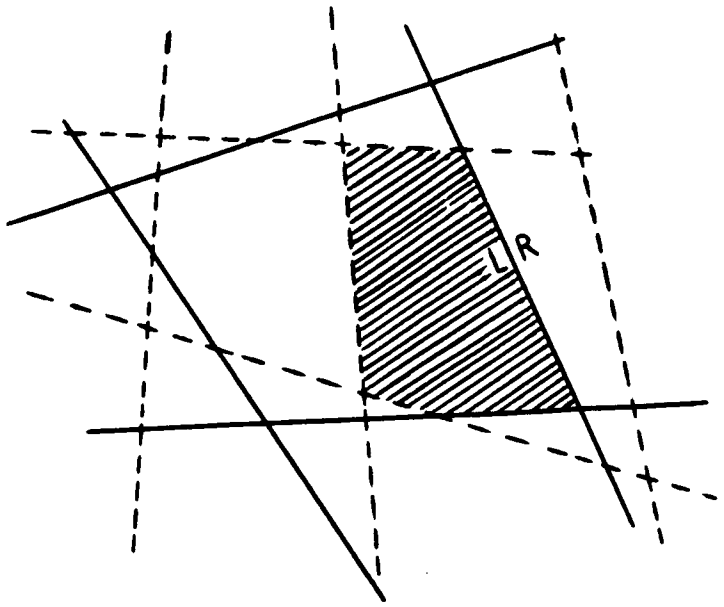

Fig. 2.2. Overlap areas arising from the superposition of the old mesh (solid lines) and the new mesh (dash lines). A typical elementary overlap area is shaded.

to be associated with the side.

The objective is to apportion a conserved quantity Q, whose volumetric density q is considered uniform within each cell of the old mesh, into the cells of the new mesh. It would be inefficient and difficult to automate in a computer, to naively sweep over the overlap areas directly. Instead, Ramshaw suggests to evaluate the same contributions by sweeping over the sides or segments s. The side or segment s is any side or segment of the polygon (overlap area). The coordinate of the two endpoints of side s will be denoted by (x_1^s, y_1^s) and (x_2^s, y_2^s).

If the side s is a segment of the old mesh, then the quantity Q in the new-mesh cell containing side s is to be incremented by an amount:

$$\Delta_s^o = \frac{1}{2} (q_L - q_R) (x_1^s, y_2^s) \text{ and } (x_2^s, y_1^s)$$

If the side s is a segment of the new mesh, then the contribution to cell on its left is $\Delta_s^N = \frac{1}{2} q_o (q_L - q_R) (x_1^s, y_2^s)$ and (x_2^s, y_1^s) while the contribution to the cell on its right is just $-\Delta_s^N$, where q_o is the volumetric density of the quantity Q of the old mesh cell in which side s lies. Adding Δ_s^o and Δ_s^N for each of the new mesh cell yields the quantity Q contained in each of the new mesh cells.

3. TWO-DIMENSIONAL HYPERBOLIC EQUATION

Consider the two-dimensional hyperbolic equation,

$$q_t + aq_x + bq_y = 0, \; 0 < x < 1, \; 0 < y < 1 \qquad (3.1a)$$

with the initial condition,

$$q(x,y,0) = f(x,y) \tag{3.1b}$$

The exact solution of Eq. 3.1 can be found as

$$q(x,y,t) = f(x - at,\ y - bt) \tag{3.2}$$

This problem is well posed [45] if boundary conditions are specified at the boundaries where the dot product, $(a,b)\cdot \hat{n} > 0$; here $(a,b) = a\hat{e}_x + b\hat{e}_y$ and $\hat{n}$ is the unit normal at the boundaries. This problem is solved on a multiple grid system using the finite-volume approach along with the three-stage Runge-Kutta integration in time. Section 3.1 is concerned with the formulation of the 2D hyperbolic equation on the curvilinear grid system. The implementation on multiple grid system is briefly discussed in Sec. 3.2. Finally, the results and discussion on various grid configuration and initial condition are given in Sec. 3.3.

3.1 Formulation of 2D Hyperbolic Equation on Curvilinear Grid

Recall Eq. 3.1,

$$q_t + aq_x + bq_y = 0$$

Since a and b are constants, one can write Eq. 3.1 in the conservation for as [46].

$$q_t + f_x + g_y = 0 \tag{3.2}$$

where

$$f = aq,\ g = bq$$

Equation 3.2 could be solved on any (x,y) coordinates, called physical coordinates. Instead, one normally solve Eq. 3.2 on the orthogonal coordinates system, called computational coordinates [47]. Thus, equation 3.2 needs to be transformed to the computational coordinates. Even though the transformation into the computational coordinates produces some additional terms in the transformed partial differential equation (thus increases the amount of computation required), it has some advantages. Boundary conditions can be treated in the straight forward way. Also, transformed equations are solved in the simple orthogonal and possibly equal spaced region. Severe departure from orthogonality will introduce truncation error in difference expressions [47]. Figure 3.1 illustrates the physical versus computational domain in a two-dimensional space. By using the chain rule, Eq. (3.2) is written as:

$$q_t + (f_\xi \xi_x + g_\xi \xi_y) + (f_\eta \eta_x + g_\eta \eta_y) = 0 \qquad (3.3)$$

Also using the chain rule, one can write:

$$dx = x_\xi d\xi + x_\eta d\eta$$
$$dy = y_\xi d\xi + y_\eta d\eta$$

which can be written in the matrix form as:

$$\begin{bmatrix} dx \\ dy \end{bmatrix} = \begin{bmatrix} x_\xi & x_\eta \\ y_\xi & y_\eta \end{bmatrix} \begin{bmatrix} d\xi \\ d\eta \end{bmatrix}$$

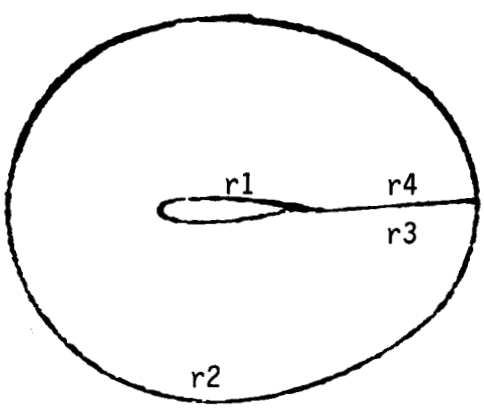

Physical Domain

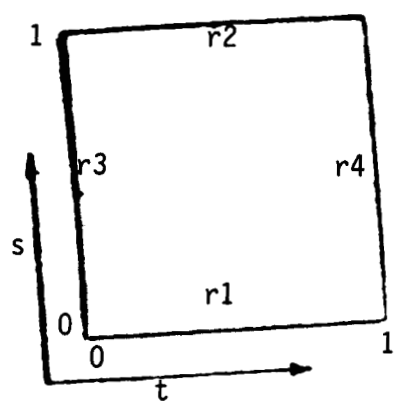

Computational Domain

Fig. 3.1. Physical vs. Computational Domain

The inversion of the matrix yields:

$$\begin{bmatrix} d\xi \\ d\eta \end{bmatrix} = \begin{bmatrix} x_\xi & x_\eta \\ y_\xi & y_\eta \end{bmatrix} \begin{bmatrix} dx \\ dy \end{bmatrix} \tag{3.4}$$

Similarly,

$$d\xi = \xi_x dx + \xi_y dy$$

$$d\eta = \eta_x dx + \eta_y dy$$

$$\begin{bmatrix} d\xi \\ d\eta \end{bmatrix} = \begin{bmatrix} \xi_x & \xi_y \\ \eta_x & \eta_y \end{bmatrix} \begin{bmatrix} dx \\ dy \end{bmatrix} \tag{3.5}$$

From Eqs. 3.4 and 3.5, it can be seen that:

$$\begin{bmatrix} \xi_x & \xi_y \\ \eta_x & \eta_y \end{bmatrix} = \begin{bmatrix} x_\xi & x_\eta \\ y_\xi & y_\eta \end{bmatrix} = \frac{1}{x_\xi y_\eta - y_\xi x_\eta} \begin{bmatrix} x_\eta & -x_\eta \\ -y_\xi & x_\xi \end{bmatrix} = J \begin{bmatrix} y_\eta & -x_\eta \\ -y_\xi & x_\xi \end{bmatrix} \tag{3.6}$$

where

$$J = \frac{1}{x_\xi y_\eta - y_\xi x_\eta} \tag{3.6a}$$

is the Jacobian of transformation. Obviously, Eq. 3.6 exists when $J \neq \infty$ or $\frac{1}{J} = \begin{bmatrix} x_\xi & x_\eta \\ y_\xi & y_\eta \end{bmatrix} \neq 0$.

From Eq. 3.6 it is found that

$$\xi_x = Jy_\eta \quad \xi_y = -Jx_\eta$$

$$\eta_x = Jy_\xi \quad \eta_y = Jx_\xi \tag{3.6b}$$

Equation 3.3 can be written as:

$$\frac{1}{J} q_t + \left[\frac{1}{J}(f\xi_x + g\xi_y)\right]_\xi + \left[\frac{1}{J}(fn_x + gn_y)\right]_n = 0 .$$

$$q_t + f_\xi + g_n = 0 \qquad (3.7)$$

$$q = q/J$$

$$f = \frac{1}{J}(f\xi_x + g\xi_y) = fy_n - gx_n \qquad (3.7a)$$

$$g = \frac{1}{J}(fn_x + gn_y) = -fy_\xi + gx_\xi$$

Equation 3.7 is the transformed equation which is solved on the computational coordinates.

3.1.1 Difference Equation

In this section, the finite volume approach is applied to Eq. 3.7 along with three-stage Runge-Kutta integration in time. The formulation of the difference equations on the equally spaced in each direction (ξ - η), computational domain is given below.

Consider a computational cell illustrated in Fig. 3.2. Recall Eq. 3.7

$$q_t + f_\xi + g_n = 0$$

$$q_t = -f_\xi - g_n$$

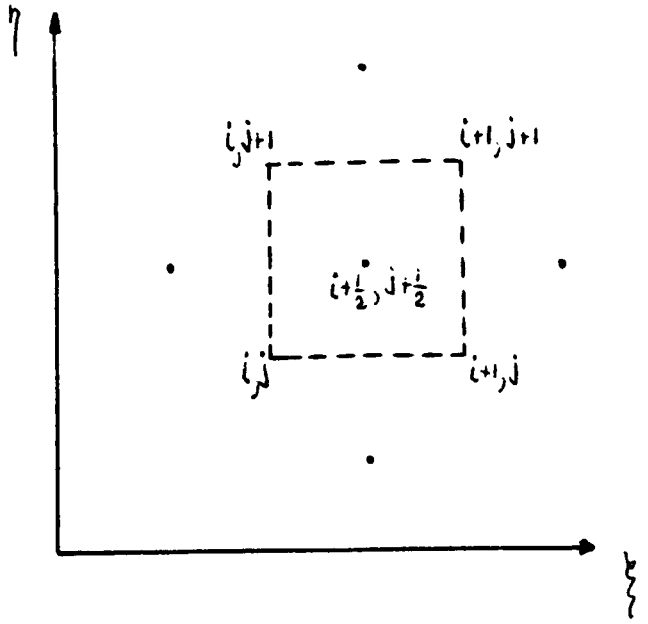

Fig. 3.2. A typical two-dimensional element.

Integrating over the cell yields

$$\int_E \hat{q}_t dE = - \int_E (\hat{f}_\xi + \hat{g}_\eta) dE.$$

Using the divergence theorem, one obtains

$$\int_E \hat{q}_t dE = -(\int_C \hat{f}_\xi \vec{n} \cdot \vec{ds} + \int_C \hat{q}_\eta \vec{n} \cdot \vec{ds})$$

Applying this to Fig. 3.2, one can write

$$\Delta\xi \, \Delta\eta \hat{q}_t \Big|_{i+\frac{1}{2}, j+\frac{1}{2}} = -\Delta\eta (\hat{f}_{i+1, j+\frac{1}{2}} - \hat{f}_{i, j+\frac{1}{2}})$$

$$-\Delta\xi (\hat{g}_{i+\frac{1}{2}, j+1} - \hat{g}_{i+\frac{1}{2}, j})$$

$$\frac{1}{J} q_t \Big|_{i+\frac{1}{2}, j+\frac{1}{2}} = \frac{-1}{\Delta\xi} (\hat{f}_{i+1, j+\frac{1}{2}} - \hat{f}_{i, j+\frac{1}{2}})$$

$$\frac{-1}{\Delta\eta} (\hat{g}_{i+\frac{1}{2}, j+1} - \hat{g}_{i+\frac{1}{2}, j})$$

$$q_t \Big|_{i+\frac{1}{2}, j+\frac{1}{2}} = J \Big|_{i+\frac{1}{2}, j+\frac{1}{2}} \quad \frac{-1}{\Delta\xi} (\hat{f}_{i+1, j+\frac{1}{2}} - \hat{f}_{i, j+\frac{1}{2}})$$

$$\frac{-1}{\Delta\eta} (\hat{g}_{i+\frac{1}{2}, j+1} - \hat{g}_{1+\frac{1}{2}, j})$$

$$= f(q^n) \qquad (3.8)$$

Each term on the right hand side of Eq. 3.8 can be written as

$$\hat{f}_{i,\, j+\frac{1}{2}} = (fy_\eta - gx_\eta)_{i+1,\, j+\frac{1}{2}}$$

$$= a(y_{i,\, j+1} - y_{i,j}) - b(x_{i,\, j+1} - x_{i,\, j}) \frac{q_{i,\, j+\frac{1}{2}}}{\Delta\eta}$$

$$\hat{g}_{i+\frac{1}{2},\, j} = (-fy_\xi + g_\xi)_{i+\frac{1}{2},\, j}$$

$$= -a(y_{i+1,\, j} - y_{i,\, j}) + b(x_{i+1,\, j} - x_{i,\, j}) \frac{q_{i+\frac{1}{2},\, j}}{\Delta\xi}$$

$$q_{i,\, j+\frac{1}{2}} = \frac{1}{2}\left(q_{i+\frac{1}{2},\, j+\frac{1}{2}} + q_{i-\frac{1}{2},\, j+\frac{1}{2}}\right) ; \; q_{i+\frac{1}{2},\, j}$$

$$= \frac{1}{2}\left(q_{i+\frac{1}{2},\, j+\frac{1}{2}} + q_{i+\frac{1}{2},\, j-\frac{1}{2}}\right)$$

$$\frac{1}{J}\Big|_{i+\frac{1}{2},\, j+\frac{1}{2}} = (x_\xi y_\eta - x_\eta y_\xi)_{i+\frac{1}{2},\, j+\frac{1}{2}}$$

$$x_\xi\Big|_{i+\frac{1}{2},\, j+\frac{1}{2}} = \frac{1}{2}\left(\frac{x_{i+1,\, j+1} - x_{i,\, j+1}}{\Delta\xi} + \frac{x_{i+1,\, j} - x_{i,\, j}}{\Delta\xi}\right)$$

$$y_\xi\Big|_{i+\frac{1}{2},\, j+\frac{1}{2}} = \frac{1}{2}\left(\frac{y_{i+1,\, j+1} - y_{i,\, j+1}}{\Delta\xi} + \frac{y_{i+1,\, j} - y_{i,\, j}}{\Delta\xi}\right)$$

$$x_\eta \Big|_{i+\frac{1}{2},\, j+\frac{1}{2}} = \frac{1}{2}\left(\frac{x_{i+1,\,j+1} - x_{i+1,\,j}}{\Delta\eta} + \frac{x_{i,\,j+1} - x_{i,\,j}}{\Delta\eta}\right)$$

$$y_\eta \Big|_{i+\frac{1}{2},\, j+\frac{1}{2}} = \frac{1}{2}\left(\frac{y_{i+1,\,j+1} - y_{i+1,\,j}}{\Delta\eta} + \frac{y_{i,\,j+1} - y_{i,\,j}}{\Delta\eta}\right)$$

The exact boundary conditions, $q(x_1, y_1, t) = f(x_1 - at, y_1 - bt)$, are given where the product $(a, b) \cdot n > 0$, and the extrapolated values of q are given at the boundaries where $(a, b) \cdot n < 0$. This is due to the nature of the hyperbolic equations.

3.1.2 Three-Stage Runge-Kutta Integration

Recall that Eq. 3.8 is written as

$$q_t \Big|_{i+\frac{1}{2},\, j+\frac{1}{2}} = f(q^n)$$

where

$$q^n = q(t_n)_{\,i+\frac{1}{2},\, j+\frac{1}{2}}$$

By applying three-stage Runge-Kutta, one may express:

$$q^{n+1*} = q^n + \Delta t f(q^n)$$

$$q^{n+1**} = q^n + \frac{1}{2}\Delta t f(q^n) + \frac{1}{2}\Delta t f(q^{n+1*})$$

$$q^{n+1} = q^n + \frac{1}{2}\Delta t f(q^n) + \frac{1}{2}\Delta t f(q^{n+1**})$$

3.2 Implementation on Multiple Grid System

As mentioned previously, for multiple grid system, the interpolation of flux will yield a conservative scheme. For the scalar 2D hyperbolic equation, Eq. 3.1, q itself is the flux transporting in time. For this problem, the difference equations as described in Sec. 3.1.1 are solved on one grid system from initial time t = 0 up to some time, say $t = t_1$. Then, at $t = t_1$ the grid system is changed and the difference equations are solved on this new grid system. The initial conditions for the new grid system are obtained by the interpolation of the final values in the old grid system, i.e., $q(x,y,t_1)$. Ramshaw's technique, as described in Sec. 2, is implemented in doing so. The results at $t = t_{final}$ are compared with the exact solutions and with the solutions obtained by using the new grid system for all time, i.e., from t = 0 to $t = _{final}$ without changing the grid system.

3.3 Results and Discussion

Various grid systems, as shown in Figs. 3.3 - 3.5, and initial conditions are implemented as described in Sec. 3.2. The results are compared with the exact solutions and the solutions obtained by using the second grid system for all time. For the case of exponentially stretching,

$$x = \frac{e^{k_1\xi} - 1}{e^{k_1} - 1}, \quad y = \frac{e^{k_2\eta} - 1}{e^{k_2} - 1}$$

the derivative contained in the Jacobian of transformation, J, x_ξ, x_η, etc. can be computed analytically. Here, results using both analytically

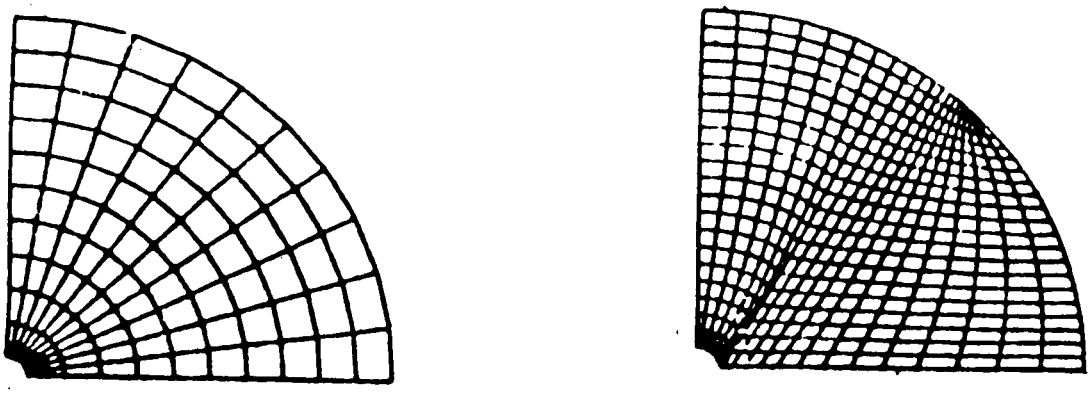

Fig. 3.3. Grid systems for a circular geometry using 11 x 11 and 21 x 21 grids.

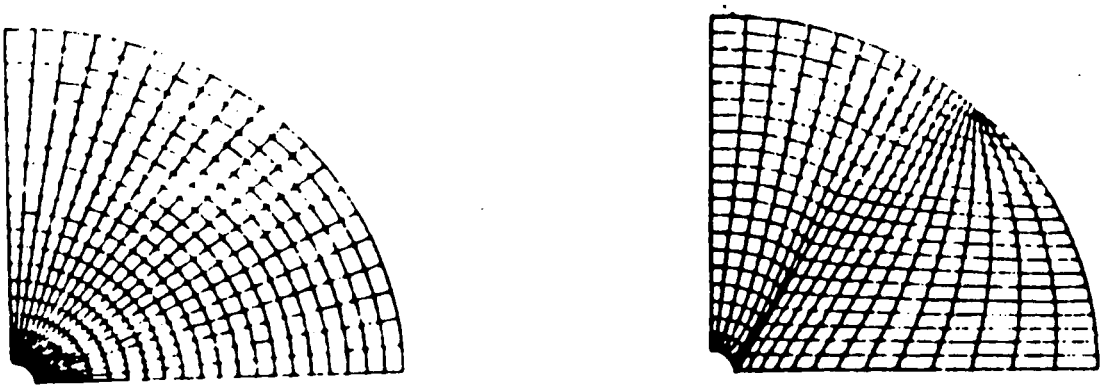

Fig. 3.4. Grid systems for a circular geometry using 21 x 21 and 21 x 21 grids.

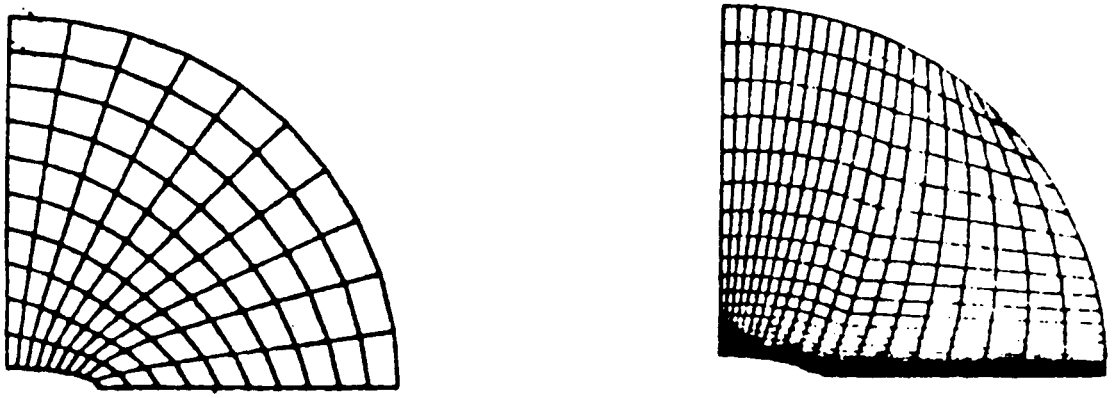

Fig. 3.5. Grid systems for an elliptic geometry using 11 x 11 and 21 x 21 grids.

computed derivatives and numerically computed derivatives are shown.

Before discussing any results, it should be noted that some error should be expected since Ramshaw's technique assumes constant volumetric density of the conserved quantity in each grid cell. But in this study, the analytic initial conditions which vary within grid cells have been selected. However, the objective of this study is to determine whether the errors grow significantly as Ramshaw's idea is implemented.

Tables 3.1 and 3.2 show the root mean square errors at final time, $t = t$ (both tables are at 200 time steps). If errors are defined as the difference between the calculated solutions and the exact solutions. the root mean square errors can be obtained as

$$\text{rms. error} = \sqrt{\frac{\Sigma \text{error}^2}{M \times N}}$$

where m x n are the number of cells contained in the grid system where the errors are computed.

Tables 3.1 and 3.2 indicate that the technique does not introduce significant errors to the solutions. The errors introduced by the technique can be seen clearly by looking at the top row of Table 3.2. In the case of constant mesh size with linear initial conditions, the finite volume calculation should yield the exact solutions. Note that multiple grid calculations even yield smaller errors than the single grid calculation in some cases. Thus, it can be concluded that the technique does not introduce significant errors to the solutions, especially when it is implemented on two grid systems which contain grid cells of comparative sizes.

Table 3.1 Root Mean Square Errors, 2D Case 1

initial conditions, $q = A\cos(\frac{\pi}{2}x)\sin(\frac{\pi}{2}y)$

exact solutions, $q = A\cos(\frac{\pi}{2}(x-at))\sin(\frac{\pi}{2}(y-bt))$

1 grid vs. 2 grid	m x n 1 grid	m x n 2 grid	rms.error 1 grid	rms.error 2 grid	rms.error multiple grid
constant mesh size	11x11	21x21	.0110307	.0027987	.0029005
expo anal.	11x11	21x21	.028259	.007452	.007656
k=1.5 num.	11x11	21x21	.02815	.007414	.00762
Fig 3.3a vs. 3.3b	11x11	21x21	.0216039	.009214	.0102846
Fig 3.4a vs. 3.4b	21x21	21x21	.002740	.009214	.009668
Fig 3.5a vs. 3.5b	11x11	21x21	.0241553	.0099474	.0108937

Table 3.2 Root Mean Square Errors, 2D Case 2

initial conditions, q = A+x+y

exact solutions, q = A+(x-at)+(y-bt)

1 grid vs. 2 grid	m x n 1 grid	m x n 2 grid	rms.error 1 grid	rms.error 2 grid	rms.error multiple grid
constant mesh size	11x11	21x21	.0000001	.0000000	.0009590
expo anal.	11x11	21x21	.0067252	.0017874	.0020591
k=1.5 num.	11x11	21x21	.0064324	.0016984	.0019984
Fig 3.3b vs.	11x11	21x21	.0025948	.0052553	.0075165
Fig 3.3a & 3.4a	21x21	21x21	.0006518	.0052553	.0053213
Fig 3.5a vs. 3.5b	11x11	21x21	.0052474	.0042585	.0043775

4. THREE-DIMENSIONAL HYPERBOLIC EQUATION

Consider the three-dimensional hyperbolic equation,

$$q_t + aq_x + bq_y + cq_z = 0 \quad 0 < x < 1,\ 0 < y < 1,\ 0 < z < 1$$

with the initial condition,

$$q(x, y, z, 0) = f(x, y, z)$$

The exact solution of this equation can be found as

$$q(x, y, z, t) = f(x-at, y-bt, z-ct)$$

As mentioned in Sec. 3, this problem is well posed if one specifies the boundary conditions at the boundaries where the dot product $(a,b,c) \cdot \vec{n} > 0$, where $(a,b,c) = a\vec{e}_x + b\vec{e}_y + c\vec{e}_z$ and $\vec{n}$ is the unit normal at the boundaries.

This problem is solved on the multiple grid system using the finite-volume approach along with the three-stage Runge-Kutta integration in time. In Sec. 4.1, the formulation of the 3D hyperbolic equation on the curvilinear grid system is described. The brief discussion on the implementation on the multiple grid is given in Sec. 4.2. Section 4.3 discusses the results from various grid configurations and initial conditions. Note that the 3D hyperbolic equation is more suitable to test Ramshaw's technique. This is because most real physical computations are performed on a three dimensional space and the governing equations are similar to the 3D hyperbolic equation.

4.1 Formulation of 3D Hyperbolic Equation on Curvilinear Grid

Consider the three dimensionl hyperbolic equation,

$$q_t + aq_x + bq_y + cq_z = 0 \tag{4.1}$$

which can be written in the conservative form as [46]

$$q_t + f_x + g_y + h_z = 0 \tag{4.2}$$

where

$$f = aq,\ g = bq,\ h = cq$$

and a, b, c are constants.

This section shows the formulation of the transformed equation of Eq. 4.2 on the computational coordinates (ξ-η-ζ). The advantages of transforming Eq. 4.2 into the computational coordinates were mentioned in Sec. 3.1. Figure 4.1 illustrates the physical versus computational domain.

By using the chain rule, Eq. 4.2 is written as

$$q_t + (f_\xi \xi_x + g_\xi \xi_y + h_\xi \xi_z) + (f_\eta \eta_x + g_\eta \eta_y + h_\eta \eta_z)$$

$$+ (f_\zeta \zeta_x + g_\zeta \zeta_y + h_\zeta \zeta_z) = 0.$$

After some mathematics manipulations, one can write

$$\left(\frac{1}{J} q\right)_t + \left(\frac{1}{J}\xi_x f + \frac{1}{J}\xi_y g + \frac{1}{J}\xi_z h\right)_\xi + \left(\frac{1}{J}\eta_x f + \frac{1}{J}\eta_y g + \frac{1}{J}\eta_z h\right)_\eta$$

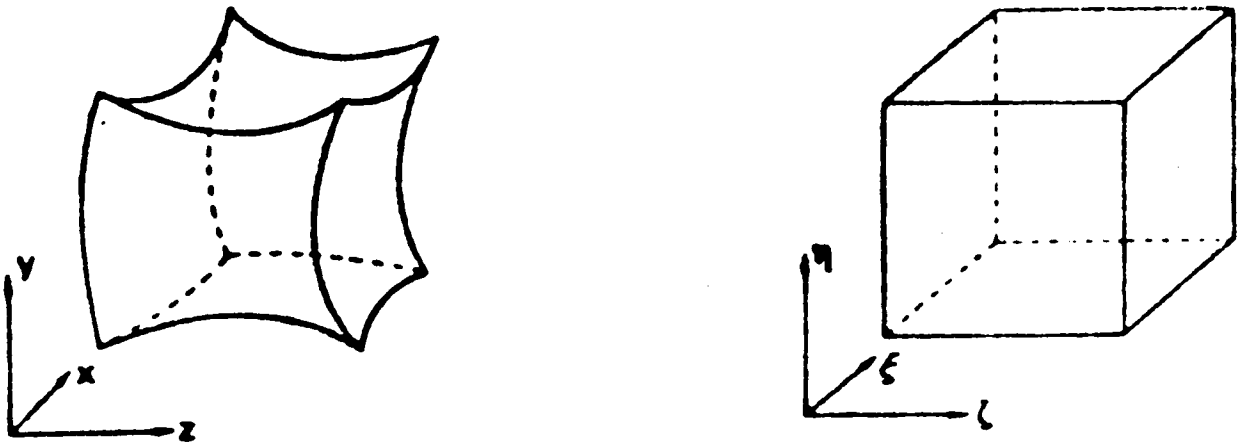

Physical Domain

Computational Domain

Fig. 4.1. Physical vs. Computational Domain.

$$+ \left(\frac{1}{J}\zeta_x f + \frac{1}{J}\zeta_y g + \frac{1}{J}\zeta_z h\right)_\zeta = 0 \qquad (4.3)$$

where

$$\begin{vmatrix} \xi_x & \xi_y & \xi_y \\ \eta_x & \eta_y & \eta_z \\ \zeta_x & \zeta_y & \zeta_z \end{vmatrix} = \left| \begin{bmatrix} x_\xi & x_\eta & x_\zeta \\ y_\xi & y_\eta & y_\zeta \\ z_\xi & z_\eta & z_\zeta \end{bmatrix}^{-1} \right|$$

Similar to Eq. 3.6, one can see that

$$\frac{1}{J}\begin{bmatrix} \xi_x & \xi_y & \xi_y \\ \eta_x & \eta_y & \eta_z \\ \zeta_x & \zeta_y & \zeta_z \end{bmatrix} = \frac{1}{J}\begin{bmatrix} x_\xi & x_\eta & x_\zeta \\ y_\xi & y_\eta & y_\zeta \\ z_\xi & z_\eta & z_\zeta \end{bmatrix}^{-1}$$

$$\frac{1}{J}\xi_x = y_\eta z_\zeta - z_\eta y_\zeta, \quad \frac{1}{J}\eta_x = -(y_\xi z_\zeta - z_\xi y_\zeta), \quad \frac{1}{J}\zeta_x = y_\xi z_\eta - z_\xi y_\eta$$

$$\frac{1}{J}\xi_y = -(x_\eta z_\zeta - z_\eta x_\zeta), \quad \frac{1}{J}\eta_y = x_\xi z_\zeta - z_\xi x_\zeta, \quad \frac{1}{J}\zeta_y = -(y_\xi z_\eta - z_\xi y_\eta)$$

$$\frac{1}{J}\xi_z = x_\eta y_\zeta - y_\eta x_\zeta, \quad \frac{1}{J}\eta_z = -(x_\xi y_\zeta - y_\xi x_\zeta), \quad \frac{1}{J}\zeta_z = x_\xi y_\eta - y_\xi x_\eta$$

Equation 4.3 can be written as

$$\hat{q}_t + \hat{f}_\xi + \hat{g}_\eta + \hat{h}_\zeta = 0 \qquad (4.4)$$

where

$$\hat{q} = \frac{q}{J}$$

$$\hat{f} = \frac{1}{J}(\xi_x f + \xi_y g + \xi_z h) = (y_\eta z_\zeta - z_\eta y_\zeta)f - (x_\eta z_\zeta - z_\eta x_\zeta)g + (x_\eta y_\zeta - y_\eta x_\zeta)h$$

$$\hat{g} = \frac{1}{J}(\eta_x f + \eta_y g + \eta_z h) = -(y_\xi z_\zeta - z_\xi y_\zeta)f + (x_\xi z_\zeta - z_\xi x_\zeta)g - (x_\xi y_\zeta - y_\xi x_\zeta)h$$

$$\hat{h} = \frac{1}{J}(\zeta_x f + \zeta_y g + \zeta_z h) = (y_\xi z_\eta - z_\xi y_\eta)f - (x_\xi z_\eta - z_\xi x_\eta)g + (x_\xi y_\eta - y_\xi x_\eta)h$$

Equation 4.4 is the transformed equation which is solved on the computational coordinate (ξ,η,ζ).

4.1.1 Difference Equation

Figure 4.2 illustrates a volume element on the computational coordinates. The difference equations are derived by applying the finite volume approach to Eq. 4.4 with the volume element as in Fig. 4.2. The details of the formulation are given below.

Recall Eq. 4.4,

$$\hat{q}_t + \hat{f}_\xi + \hat{g}_\eta + \hat{h}_\zeta = 0$$

or

$$\hat{q}_t = -\hat{f}_\xi - \hat{g}_\eta - \hat{h}_\zeta$$

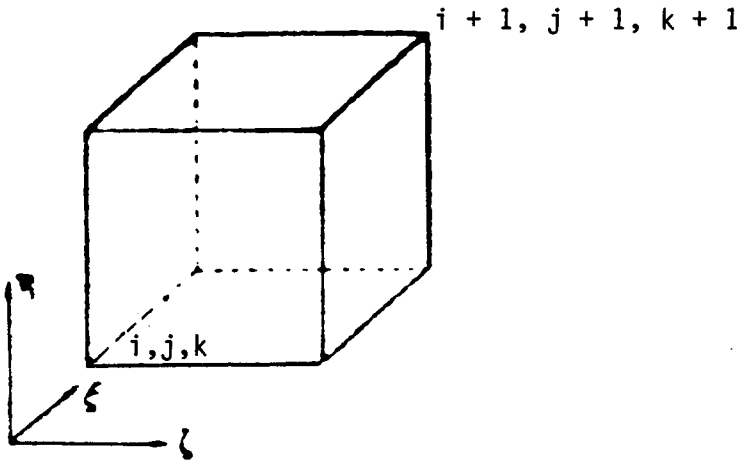

Fig. 4.2. A typical volume element.

Integrating over the volume element, it is expressed as

$$\int_{\forall} \hat{q}_t \, dV = -\int_{\forall} (\hat{f}_{\xi} + \hat{g}_{\eta} + \hat{h}_{\zeta}) \, dV$$

Applying the divergence theorem to the right hand side, the above equation can be written as

$$\int_{\forall} \hat{q}_t \, dV = -\left(\int_A \hat{f}_{\xi} \cdot \vec{dA} + \int_A \hat{g}_{\eta} \cdot \vec{dA} + \int_A \hat{h}_{\zeta} \cdot \vec{dA}\right)$$

Utilizing Fig. 4.2, the difference equation for the above equation can be written as

$$\begin{aligned} \Delta\xi\Delta\eta\Delta\zeta \hat{q}_t \Big|_{i+\frac{1}{2},\, j+\frac{1}{2},\, k+\frac{1}{2}} = & -\Delta\eta\Delta\zeta(\hat{f}_{i+1,\, j+\frac{1}{2},\, k+\frac{1}{2}} \\ & - \hat{f}_{i,\, j+\frac{1}{2},\, k+\frac{1}{2}}) \\ & -\Delta\xi\Delta\zeta(\hat{g}_{i+\frac{1}{2},\, j+1,\, k+\frac{1}{2}} \\ & - \hat{g}_{i+\frac{1}{2},\, j,\, k+\frac{1}{2}}) \\ & -\Delta\xi\Delta\eta(\hat{h}_{i+\frac{1}{2},\, j+\frac{1}{2},\, k+1} \\ & - \hat{h}_{i+\frac{1}{2},\, j+\frac{1}{2},\, k}) \end{aligned} \qquad (4.5)$$

where, $\hat{f}_{i,\, j+\frac{1}{2},\, k+\frac{1}{2}} = [(y_\eta z_\zeta - z_\eta y_\zeta) f - (x_\eta z_\zeta - z_\eta x_\zeta) g + (x_\eta y_\zeta - y_\eta x_\zeta) h]_{i,\, j+\frac{1}{2},\, k+\frac{1}{2}}$

$$x_\eta \Big|_{i,\, j+\frac{1}{2},\, k+\frac{1}{2}} = \frac{1}{2}\left(\frac{x_{i,\, j+1,\, k} - x_{i,\, j,\, k}}{\Delta\eta} + \frac{x_{i,\, j+1,\, k+1} - x_{i,\, j,\, k+1}}{\Delta\eta}\right)$$

$$y_\eta \Big|_{i,\, j+\frac{1}{2},\, k+\frac{1}{2}} = \frac{1}{2}\left(\frac{y_{i,\, j+1,\, k} - y_{i,\, j,\, k}}{\Delta\eta} + \frac{y_{i,\, j+1,\, k+1} - y_{i,\, j,\, k+1}}{\Delta\eta}\right)$$

$$z_\eta \Big|_{i,\, j+\frac{1}{2},\, k+\frac{1}{2}} = \frac{1}{2}\left(\frac{z_{i,\, j+1,\, k} - z_{i,\, j,\, k}}{\Delta\eta} + \frac{z_{i,\, j+1,\, k+1} - z_{i,\, j,\, k+1}}{\Delta\eta}\right)$$

$$x_\zeta \Big|_{i,\, j+\frac{1}{2},\, k+\frac{1}{2}} = \frac{1}{2}\left(\frac{x_{i,\, j,\, k+1} - x_{i,\, j,\, k}}{\Delta\eta} + \frac{x_{i,\, j+1,\, k+1} - x_{i,\, J+1,\, k}}{\Delta\eta}\right)$$

$$y_\zeta \Big|_{i,\, j+\frac{1}{2},\, k+\frac{1}{2}} = \frac{1}{2}\left(\frac{y_{i,\, j,\, k+1} - y_{i,\, j+1,\, k}}{\Delta\zeta} + \frac{y_{i,\, j+1,\, k+1} - y_{i,\, j,\, k}}{\Delta\zeta}\right)$$

$$z_\zeta \Big|_{i,\, j+\frac{1}{2},\, k+\frac{1}{2}} = \frac{1}{2}\left(\frac{z_{i,\, j,\, k+1} - z_{i,\, j,\, k}}{\Delta\zeta} + \frac{z_{i,\, j+1,\, k+1} - z_{i,\, j+1,\, k}}{\Delta\zeta}\right)$$

$$\hat{q}_{i+\frac{1}{2},\,j,\,k+\frac{1}{2}} = [-(y_\xi z_\zeta - z_\xi y_\zeta)f + (x_\xi z_\zeta - z_\xi x_\zeta)g - (x_\xi y_\zeta - y_\xi x_\zeta)h]_{i+\frac{1}{2},\,j,\,k+\frac{1}{2}}$$

$$x_\xi\Big|_{i+\frac{1}{2},\,j,\,k+\frac{1}{2}} = \frac{1}{2}\left(\frac{x_{i+1,\,j,\,k} - x_{i,\,j,\,k}}{\Delta\xi} + \frac{x_{i+1,\,j,\,k+1} - x_{i,\,j,\,k+1}}{\Delta\xi}\right)$$

$$y_\xi\Big|_{i+\frac{1}{2},\,j,\,k+\frac{1}{2}} = \frac{1}{2}\left(\frac{y_{i+1,\,j,\,k} - y_{i,\,j,\,k}}{\Delta\xi} + \frac{y_{i+1,\,j,\,k+1} - y_{i,\,j,\,k+1}}{\Delta\xi}\right)$$

$$z_\xi\Big|_{i+\frac{1}{2},\,j,\,k+\frac{1}{2}} = \frac{1}{2}\left(\frac{z_{i+1,\,j,\,k} - z_{i,\,j,\,k}}{\Delta\xi} + \frac{z_{i+1,\,j,\,k+1} - z_{i,\,j,\,k+1}}{\Delta\xi}\right)$$

$$x_\zeta\Big|_{i+\frac{1}{2},\,j,\,k+\frac{1}{2}} = \frac{1}{2}\left(\frac{x_{i,\,j,\,k+1} - x_{i,\,j,\,k}}{\Delta\zeta} + \frac{x_{i+1,\,j,\,k+1} - x_{i+1,\,j,\,k}}{\Delta\zeta}\right)$$

$$y_\zeta\Big|_{i+\frac{1}{2},\,j,\,k+\frac{1}{2}} = \frac{1}{2}\left(\frac{y_{i,\,j,\,k+1} - y_{i,\,j,\,k}}{\Delta\zeta} + \frac{y_{i+1,\,j,\,k+1} - y_{i+1,\,j,\,k}}{\Delta\zeta}\right)$$

$$z_\zeta \Big|_{i+\frac{1}{2},\, j,\, k+\frac{1}{2}} = \frac{1}{2}\left(\frac{z_{i,\,j,\,k+1} - z_{i,\,j,\,k}}{\Delta\zeta} + \frac{z_{i+1,\,j,\,k+1} - z_{i+1,\,j,\,k}}{\Delta\zeta}\right)$$

$$\hat{h}_{i+\frac{1}{2},\, j+\frac{1}{2},\, k} = \left[(y_\xi z_\eta - z_\xi y_\eta)f - (x_\xi z_\eta - z_\xi x_\eta)g + (x_\xi y_\eta - y_\xi x_\eta)h\right]_{i+\frac{1}{2},\, j+\frac{1}{2},\, k}$$

$$x_\xi \Big|_{i+\frac{1}{2},\, j+\frac{1}{2},\, k} = \frac{1}{2}\left(\frac{x_{i+1,\,j,\,k} - x_{i,\,j,\,k}}{\Delta\xi} + \frac{x_{i+1,\,j+1,\,k} - x_{i,\,j+1,\,k}}{\Delta\xi}\right)$$

$$y_\xi \Big|_{i+\frac{1}{2},\, j+\frac{1}{2},\, k} = \frac{1}{2}\left(\frac{y_{i+1,\,j,\,k} - y_{i,\,j,\,k}}{\Delta\xi} + \frac{y_{i+1,\,j+1,\,k} - y_{i,\,j+1,\,k}}{\Delta\xi}\right)$$

$$z_\xi \Big|_{i+\frac{1}{2},\, j+\frac{1}{2},\, k} = \frac{1}{2}\left(\frac{z_{i+1,\,j,\,k} - z_{i,\,j,\,k}}{\Delta\xi} + \frac{z_{i+1,\,j+1,\,k} - z_{i,\,j+1,\,k}}{\Delta\xi}\right)$$

$$x_\eta \Big|_{i+\frac{1}{2},\, j+\frac{1}{2},\, k} = \frac{1}{2}\left(\frac{x_{i,\,j+1,\,k} - x_{i,\,j,\,k}}{\Delta\eta} + \frac{x_{i+1,\,j+1,\,k} - x_{i+1,\,j,\,k}}{\Delta\eta}\right)$$

$$y_\eta \Big|_{i+\frac{1}{2},\, j+\frac{1}{2},\, k} = \frac{1}{2}\left(\frac{y_{i,\, j+1,\, k} - y_{i,\, j,\, k}}{\Delta\eta} + \frac{y_{i+1,\, j+1,\, k} - y_{i+1,\, j,\, k}}{\Delta\eta}\right)$$

$$z_\eta \Big|_{i+\frac{1}{2},\, j+\frac{1}{2},\, k} = \frac{1}{2}\left(\frac{z_{i,\, j+1,\, k} - z_{i,\, j,\, k}}{\Delta\eta} + \frac{x_{i+1,\, j+1,\, k} - x_{i+1,\, j,\, k}}{\Delta\eta}\right)$$

$$f = aq, \quad g = bq, \quad h = cq$$

$$q_{i,\, j+\frac{1}{2},\, k+\frac{1}{2}} = \frac{1}{2}\left(q_{i+\frac{1}{2},\, j+\frac{1}{2},\, k+\frac{1}{2}} + q_{i-\frac{1}{2},\, j+\frac{1}{2},\, k+\frac{1}{2}}\right)$$

$$q_{i+\frac{1}{2},\, j,\, k+\frac{1}{2}} = \frac{1}{2}\left(q_{i+\frac{1}{2},\, j+\frac{1}{2},\, k+\frac{1}{2}} + q_{i+\frac{1}{2},\, j-\frac{1}{2},\, k+\frac{1}{2}}\right)$$

$$q_{i+\frac{1}{2},\, j+\frac{1}{2},\, k} = \frac{1}{2}\left(q_{i+\frac{1}{2},\, j+\frac{1}{2},\, k+\frac{1}{2}} + q_{i+\frac{1}{2},\, j+\frac{1}{2},\, k-\frac{1}{2}}\right)$$

$$\hat{q} \Big|_{i+\frac{1}{2},\, j+\frac{1}{2},\, k+\frac{1}{2}} = \frac{1}{J}\, q \Big|_{i+\frac{1}{2},\, j+\frac{1}{2},\, k+\frac{1}{2}}$$

$$\frac{1}{J} \Big|_{i+\frac{1}{2},\, j+\frac{1}{2},\, k+\frac{1}{2}} = [x_\xi (y_\eta z_\zeta - z_\eta y_\zeta) - x_\eta (y_\xi z_\zeta - z_\xi y_\zeta) + x_\zeta (y_\xi z_\eta - z_\xi y_\eta)]_{i+\frac{1}{2},\, j+\frac{1}{2},\, k+\frac{1}{2}}$$

$$x_\xi \Big|_{i+\frac{1}{2},\, j+\frac{1}{2},\, k+\frac{1}{2}} = \frac{1}{2}\left[\frac{1}{2}\left(\frac{x_{i+1,j,k} - x_{i,j,k}}{\Delta\xi} + \frac{x_{i+1,j+1,k} - x_{i,j+1,k}}{\Delta\xi}\right) + \frac{1}{2}\left(\frac{x_{i+1,j,k+1} - x_{i,j,k+1}}{\Delta\xi} + \frac{x_{i+1,j+1,k+1} - x_{i,j+1,k+1}}{\Delta\xi}\right)\right]$$

$$x_\eta \Big|_{i+\frac{1}{2},\, j+\frac{1}{2},\, k+\frac{1}{2}} = \frac{1}{2}\left[\frac{1}{2}\left(\frac{x_{i,j+1,k} - x_{i,j,k}}{\Delta\eta} + \frac{x_{i+1,j+1,k} - x_{i+1,j,k}}{\Delta\eta}\right) + \frac{1}{2}\left(\frac{x_{i,j+1,k+1} - x_{i,j,k+1}}{\Delta\eta} + \frac{x_{i+1,j+1,k+1} - x_{i+1,j,k+1}}{\Delta\eta}\right)\right]$$

$$x_\zeta \Big|_{i+\frac{1}{2},\, j+\frac{1}{2},\, k+\frac{1}{2}} = \frac{1}{2}\left[\frac{1}{2}\left(\frac{x_{i,j,k+1} - x_{i,j,k}}{\Delta\zeta} + \frac{x_{i+1,j,k+1} - x_{i+1,j,k}}{\Delta\zeta}\right) + \frac{1}{2}\left(\frac{x_{i,j+1,k+1} - x_{i,j+1,k}}{\Delta\zeta} + \frac{x_{i+1,j+1,k+1} - x_{i+1,j+1,k}}{\Delta\zeta}\right)\right]$$

Similar expressions can be written for y_ξ, y_η, y_ζ, z_ξ, z_η, and z_ζ. Finally, Eq. 4.5 can be written in the form:

$$qt = f\ (q^h)$$

The three-stage Runge-Kutta integration as described in Sec. 3.1.2 can be applied here.

4.2 IMPLEMENTATION ON MULTIPLE GRID SYSTEM

Figure 4.3 illustrates an example of multiple grid used in this study. Here, the grid system changes from one to another at the plane $z = z_1$. In order to solve the difference equations, as in section 4.1.1, on this grid system, the extra boundary conditions are needed at the interface, i.e., plane $z = z_1$ where the two single grid system meet. These boundary conditions are not the physical boundary conditions. Many authors refer to them as interface conditions, for example see Berger [43]. Special treatments mush be given for these boundary conditions. Figure 4.4 shows the typical interface in this study.

In Fig. 4.4, h_o denotes the flux h coming out from the first grid system and h_n denotes the flux h going into the second grid system. Here, h_o is needed for the first grid calculations and h_n is needed for the calculations on the second grid. They are the extra boundary conditions mentioned previously. In this study, h_o is obtained by the interpolations between the first and the second grid. The flux h_n is obtained by transferring h_o across the interface using the Ramshaw's technique described in Sec. 2. The calculations begin from initial time, $t = 0$, to some time, say $t = t_{final}$. The results from the multiple grid calculations are compared with the exact solutions and the solutions obtained from the single grid calculations for various grid system and initial conditions.

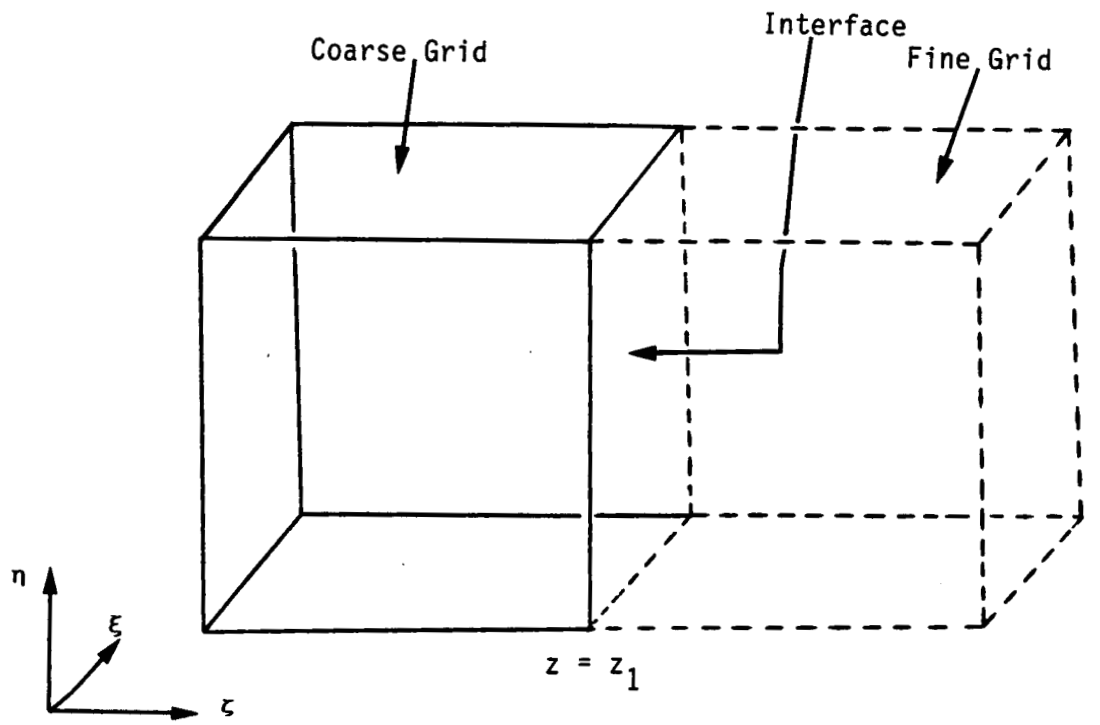

Fig. 4.3. A computational domain arising from two patched grids.

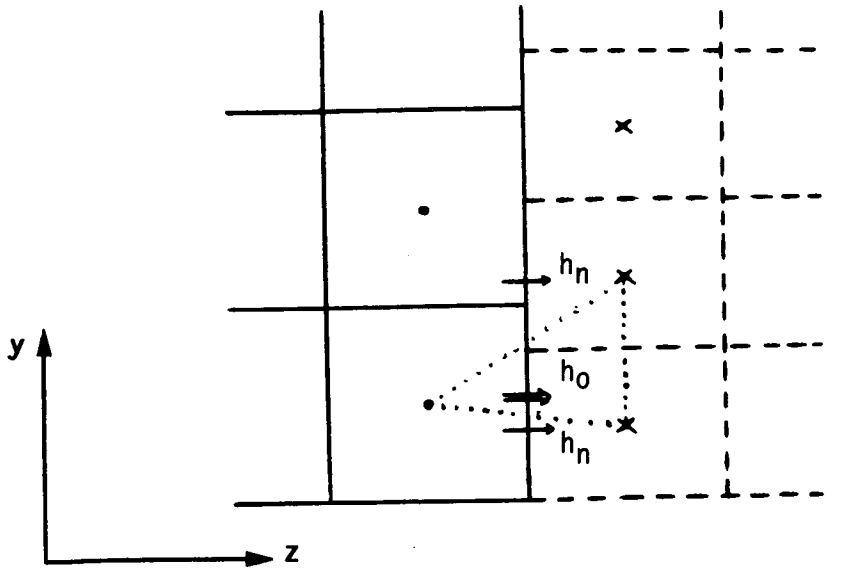

Fig. 4.4. An interface where h_o is obtained by interpolating h from the points indicated by dotted triangle and h_n is obtained by Ramshaw's technique.

4.3 RESULTS AND DISCUSSIONS

Tables 4.1 and 4.2 show the results obtained from the calculations on various grid systems with two different initial conditions. If the error is defined as the difference between the numerical solutions and the exact solutions, the root mean square error can be found as

$$\text{rms. error} = \sqrt{\frac{\sum \text{error}^2}{N}}$$

where N = total number of grid cells.

Both tables illustrate the rms. errors from the multiple grid calculations as well as the calculations from each of single grid which compose the multiple grid. Table 4.1 gives the results with linear initial conditions, while the results with trigonomitrical initial conditions are given in Table 4.2. It can be seen from both tables that the multiple grid calculation does not introduce significant errors to the over all solutions. In some cases, the multiple grid calculations even give better solutions than the calculations from the single grid.

5. CONCLUSIONS

The results from this study have shown that the technique works reasonably well when the two grid systems contain grid cells of comparative sizes. This can be clearly seen when one recalls the assumptions made for the technique, i.e., each grid cell contains uniform conserved quantity. Since, in general, this criterion cannot be met in the real physical calculations, some effort may need to be made to seek for the best possible types of grids in order to apply the technique. It should be pointed out that only simple

Table 4.1 Root Mean Square Errors, 3D Case 1.

initial conditions, q = A+x+y+z

exact solutions, q = A+(x-at)+(y-bt)+(z-ct)

configuration	No. of pts. 1st vs. 2nd	rms.error		
		single grid		mul. grid
		first	second	
	11x11x11 vs. 21x21x11	.000000	.000000	.013660
	21x21x11 vs. 11x11x11	.000000	.000000	.000004
	17x17x11 vs. 21x21x11	.000000	.000000	.005720
const. mesh	21x21x11 vs. 17x17x11	.000000	.000000	.003334
	19x19x11 vs. 21x21x11	.000000	.000000	.002163
	21x21x11 vs. 19x19x11	.000000	.000000	.001703
exp.streching	21x21x11 vs. 21x21x11	.000000	.002106	.002389
with k=3.0	21x21x11 vs. 21x21x11	.002106	.000000	.007139
(*=const.mesh)				
	O-type vs. H-type			
cylinder	21x21x11 vs. 21x21x11	.000608	.015882	.009620
	11x11x11 vs. 21x21x11	.002842	.012321	.012883
Butler-wing	17x17x11 vs. 21x21x11	.001495	.012321	.008672
	21x21x11 vs. 21x21x11	.001275	.012321	.008379

Table 4.2 Root Mean Square Errors, 3D Case 2

initial conditions, $q = A\cos(\frac{\pi}{2}x)\sin(\frac{\pi}{2}y)\sin(\frac{\pi}{2}z)$

exact solutions, $q = A\cos(\frac{\pi}{2}(x-at))\sin(\frac{\pi}{2}(y-bt))\sin(\frac{\pi}{2}(z-ct))$

configuration	No. of pts. 1st vs. 2nd	rms. error		
		single grid		mul. grid
		first	second	
const. mesh	11x11x11 vs. 21x21x11	.005560	.001901	.019420
	21x21x11 vs. 11x11x11	.001901	.005560	.003786
	17x17x11 vs. 21x21x11	.002494	.001901	.006363
	21x21x11 vs. 17x17x11	.001901	.002494	.004219
	19x19x11 vs. 21x21x11	.002136	.001901	.003414
	21x21x11 vs. 19x19x11	.001901	.002136	.003070
exp.streching	21x21x11* vs. 21x21x11	.001901	.004424	.005578
with k=3.0	21x21x11 vs. 21x21x11*	.004424	.001901	.008227
(*=const.mesh)				
	O-type vs. H-type			
cylinder	21x21x11 vs. 21x21x11	.001651	.021766	.011515
	11x11x11 vs. 21x21x11	.007848	.0211753	.017058
Butler-wing	17x17x11 vs. 21x21x11	.003297	.0211753	.012327
	21x21x11 vs. 21x21x11	.002180	.0211753	.011819

configurations are chosen for this study, i.e., a single grid system can be generated around these configurations. For more complex bodies, the multiple grid approach may be the only way to attack the problem if the complexity of the geometries is to be maintained.

This study demonstrates that use of the multiple grid does not introduce any significant error to the problems. The next step is to apply this technique to solve the equations of motion over an ideal aircraft configuration such as a Butler-Wing configuration (Fig. 5.1). If the results from the Butler-Wing calculations are satisfied, the next step is to consider this technique along with the equations of motion over the real aircraft configuration. It is expected that results from this study will give some contributions to the field of Computational Fluid Dynamics.

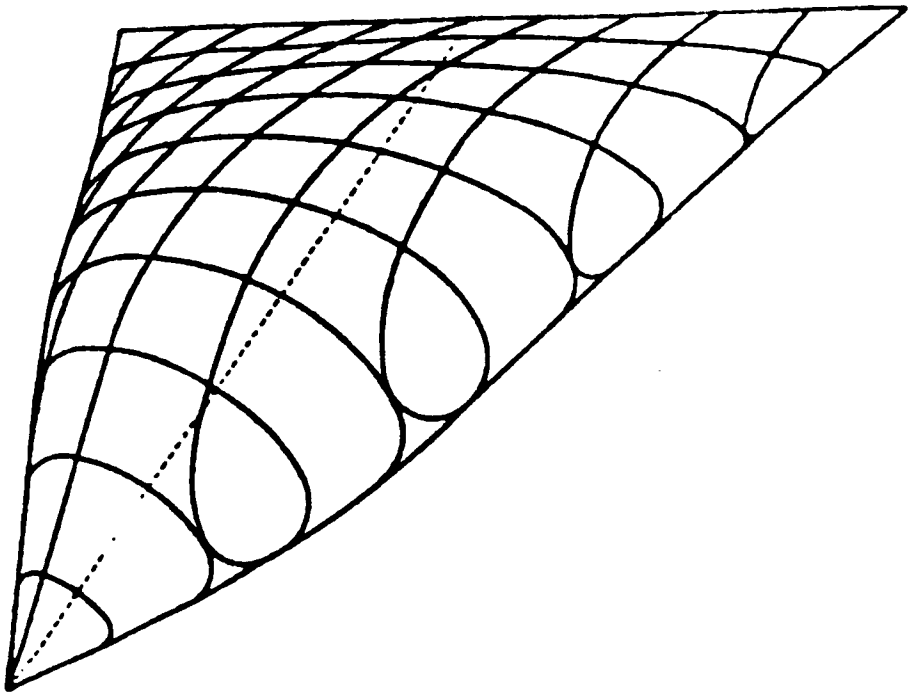

Fig. 5.1. A Butler-Wing configuration.

REFERENCES

1. Jameson, A. and Baker, T.J., "Solution of the Euler Equations for Complex Configurations," AIAA 6th Comput. Fluids Dynamics Conference, Paper 83-1929, July 1983, pp. 293-302.

2. Atta, E., "Component-Adaptive Grid Interfacing," AIAA 19th Aerospace Sciences Meeting, Paper 81-0382, January 1981.

3. Benek, J.A., Steger, J.L., and Dougherty, F.C., "A Flexible Grid Embedding Technique with Application to the Euler Equations," AIAA 6th Comput. Fluids Dynamics Conference, Paper 83-1944, July 1983, pp. 373-382.

4. Boppe, C., "Calculation of Transonic Wing Flows by Grid Embedding," AIAA 15th Aerospace Sciences Meeting, Paper 77-207, January 1977.

5. Lax, P., "Hyperbolic Systems of Conservation Laws and the Mathematical Theory of Shock Waves," SIAM, 1972.

6. Warming, R. and Beam, R., "Upwind Second-Order Difference Schemes and Applications in Aerodynamic Flows," AIAA Journal Volume 14, September 1976, pp. 1241-1249.

7. Hessenius, K. and Pulliam, T., "A Zonal Approach to Solution of the Euler Equations," AIAA/ASME 3rd Joint Thermophysics, Fluids, Plasma and Heat Transfer Conference, Paper 82-0369, June 1982.

8. Rai, M.M., "A Conservative Treatment of Zonal Boundaries for Euler Equation Calculations," AIAA 22nd Aerospace Sciences Meeting, paper 84-0164, January 1984.

9. Cambier, L., Ghazzi, W., Veuillot, J.P., and Viviand, H., "Une Approache par Domaines pour le Calcu d'Ecoulements Compressibles," Cinquieme Colloque International sur les Methodes de calcu, France, December 1981.

10. Rai, M.M., Chakravarthy, S.R., and Hessenius, K.A., "Zonal Grid Calculations Using the Osher Scheme," International Journal of Computers and Fluids, Volume 12, No. 3, 1984, pp. 161-175.

11. Steger, J.L., Dougherty, F.C., and Benek, J.A., "A Chimera Grid Scheme," Mini-Symposium on Advances in Grid Generations, ASME Applied, Bioengineering and Fluids Engineering Conference, Houston, Texas, June 1983.

12. Beam, R. and Warming, R., "An implicit Factored Scheme for the Compressible Navier-Stokes Equations," AIAA Journal, Volume 16, April 1978, pp. 393-402.

13. Atta, E. and Vadyak, J., "A Grid Interfacing Algorithm for Three-Dimensional Transonic Flows and Aircraft Configurations," AIAA/ASME 3rd

Joint Thermophysics, Fluids, Plasma and Heat Transfer Conference, Paper 82-1017, June 1982.

14. Osher, S. and Sanders, R., "Numerical Approximations to Nonlinear Conservation Laws with Locally Varying Time and Space Grids," Math. Comp., Volume 41, September 1983, pp. 321-336.

15. Berger, M.J., "Stability of Interfaces with Mesh Refinement," ICASE/NASA/Langley Research Center, Hampton, Virginia, Report No. 83-42, August 1983.

16. Trefetnen, L.N., "Stability of Finite Difference Models Containing Two Boundaries or Interfaces," ICASE NASA/Langley Research Center, Hampton, Virginia, Report No. 84-11, March 1984.

17. Berger, M.J. and Oliger, J., "Adaptive Mesh Refinement for Hyperbolic Partial Differential Equations," Journal of Computational Physics, Volume 53, March 1984, pp. 484-512.

18. Browning, G., Kreiss, H.-O., and Oliger, J., "Mesh Refinement," Math. Comp., Volume 27, January 1973, pp. 29-39.

19. Cement, M., "Stable Difference Schemes with Uneven Mesh Spacings," Math. Comp., Volume 25, April 1971, pp. 219-226.

20. MacCamy, R.C. and Martin, S.P., "A Finite Element Method for Exterior Interface Problems," Int. J. Math. Math. Sci., Volume 3, 1980, pp.311-350.

21. Dukowicz, J.K., "Conservative Rezoning (Remapping) for General Quadrilateral Meshes," Journal of Computational Physics, Volume 54, June 1984, pp. 411-424.

22. Ramshaw, J.D., "Conservative Rezoning Algorithm for Generalized Two-Dimensional Meshes," Journal of Computational Physics, Volume 59, June 1985, pp. 193-199.

23. Harten, A., Lax, P., and Leer, B., "On Upstream Differencing and Gudunov-Type Schemes for Hyperbolic Conservation Laws," ICASE NASA/Langley Research Center, Hampton, Virginia, Report No. 82-5, March 1982.

24. Leer, B., "Multidimensional Explicit Difference Schemes for Hyperbolic Conservation Laws," ICASE NASA/Langley Research Center, Hampton, Virginia, Report No. 172254, November 1983.

25. Beam, R. and Warming, R., "An Implicit Finite Difference Algorithm for Hyperbolic Systems in the Conservation Law Form," Journal of Computational Physics, Volume 22, September 1976, pp. 87-110.

26. Turkel, E., "Composite Methods for Hyperbolic Equations," SIAM Journal of Numerical Analysis, Volume 14, September 1977, pp. 744-759.

27. Starius, G., "On Composite Mesh Difference Methods for Hyperbolic Differential Equations," Numerical Math., 1980, pp. 241-255.

28. Oliger, J., "Fourth-Order Difference Methods for the Initial-Boundary Value Problem for Hyprbolic Equations," Math. Comp. Volume 28, January 1974, pp. 15-25.

29. Oliger, J., "Hybrid Difference Methods for the Initial-Boundary Value Problem for Hyperbolic Equations," Math. Comp. Volume 30, October 1976, pp. 724-738.

30. Harten, A., "High Resolution Schemes for Hyperbolic Conservation Laws," Journal of Computational Physics, Volume 49, March 1983, pp. 357-393.

31. Gottlieb, D., Gunzburger, M., and Turkel, E., "On Numerical Boundary Treatment of Hyperbolic Systems for Finite Difference and Finite Element Methods," ICASE NASA/Langley Research Center, Hampton, Virginia, Report No. 78-13, September 1978.

32. Abarbanel, S.S. and Murman, E.M., "Stability of Two-Dimensional Hyperbolic Initial Boundary Value Problems for Explicit and Implicit Schemes," ICASE NASA/Langley Research Center, Hampton, Virginia, Report No. 81-29, August 1981.

33. Trefethen, L.N. and Halpern, L., "Well-Posedness of One-Way Wave Equations and Absorbing Boundary Condition," ICASE NASA/Langley Research Center, Hampton, Virginia, Report No. 85-30, June 1985.

34. Osher, S. and Tadmore, E., "On Convergence of Difference Approximations to Scalar Conservation Laws," ICASE NASA/Langley Research Center, Hampton, Virginia, Report No. 85-28, May 1985.

35. Goldberg, M. and Tadmor, E. "Scheme-Independent Stability Criteria for Difference Approximations of Hyperbolic Initial-Boundary Value Problems. II.," Math. Comp. Volume 36, April 1981, pp. 603-626.

36. Osher, S., "Stability of Difference Approximations of Dissipative Type for Mixed Initial-Boundary Value Problem. I.," Math. Comp., Volume 23, April 1969, pp. 335-340.

37. Trefethen, L.N., "Instability of Difference Models for Hyperbolic Initial-Boundary Value Problems," Communications on Pure and Applied Math., Volume 37, May 1984, pp. 329-367.

38. Moitra, A., Turkel, E., and Kumar, A., "Application of a Runge-Kutta Scheme for High-Speed Inviscid Internal Flows," ICASE NASA/Langley Research Center, Hampton, Virginia, Report No. 86-5, January 1986.

39. Turkel, E., "Accuracy of Schemes with Nonuniforms Meshes for Compressible Fluid Flows," ICASE NASA/Langley Research Center, Hampton, Virginia, Report No. 85-43, September 1985.

40. Turkel, E., Yaniv, S., and Landau, U., "Accuracy of Schemes for the Euler Equations with Nonuniform Meshes," ICASE NASA/Langley Research Center, Hampton, Virginia, Report No. 85-59, December 1985.

41. Jamesons, A., Schmidt, W., and Turkel, E., "Numerical Solutions of the Euler Equations by Finite Volume Methods Using Runge-Kutta Time Stepping Schemes," AIAA 14th Fluids and Plasma Dynamics Conference, Paper 81-1259, June 1981.

42. Moitra, A., "Numerical Solution of the Euler Equations for High-Speed, Blended Wing-Body Configurations," AIAA 23rd Aerospace Sciences Meeting, Paper 85-0123, January 1985.

43. Berger, M.J., "On Conservation at Grid Interfaces," ICASE NASA/Langley Research Center, Hampton, Virginia, Report No. 84-43, September 1984.

44. Rektorys, K. (Ed.), "Survey of Applicable Mathematics," p. 207, MIT Press, Cambridge, Mass. 1969.

45. Erickson, L.-E., "Transfinite Mesh Generation and Computer-Aided Analysis of Mesh Effects, Ph. D. Thesis, Department of Computer Sciences, Uppsala University, Uppsala, Sweden.

46. Anderson, D.A., Tannehill, J.C., and Pletcher, R.H., "Computational Fluid Mechanics and Heat Transfer," Hemisphere Publishing Corporation, New York, New York, 1984.

47. Thompson, J.F., Warsi, Z.U.A., and Mastin, W.C., "Numerical Grid Generation," North-Holland, New York, New York.